IEEE Access
Multidisciplinary ⋮ Rapid Review ⋮ Open Access Journal

Received 23 May 2023, accepted 8 June 2023, date of publication 13 June 2023, date of current version 19 June 2023.

Digital Object Identifier 10.1109/ACCESS.2023.3285819

RESEARCH ARTICLE

Comparative Assessment of Switching Overvoltages Suppression Measures in Different Wind Farm Topologies

TAMER ELIYAN[1,2], IBRAHIM B. M. TAHA[3], AND FADY WADIE[4]

[1]Electrical Engineering Department, Faculty of Engineering at Shoubra, Benha University, Cairo 11629, Egypt
[2]Department of Electrical Power and Machines Engineering, The Higher Institute of Engineering at El-Shorouk City, Alshorouk Academy, Cairo 11837, Egypt
[3]Department of Electrical Engineering, College of Engineering, Taif University, Taif 21944, Saudi Arabia
[4]Mechatronics and Robotics Engineering Department, Faculty of Engineering, Egyptian Russian University, Badr City 11829, Egypt

Corresponding author: Fady Wadie (engfadywadie@hotmail.com)

This work was supported by the Deanship of Scientific Research, Taif University.

ABSTRACT Mitigation techniques associating vacuum circuit breakers (VCB) were proven highly effective in reducing switching overvoltages (SOV) in wind farms. However, the structure of wind farms in modern-day power systems is not fixed to a certain topology. In this paper, the impact of changing the topology of the wind farm upon the capability of mitigation techniques in reducing SOV was investigated which is considerd the first contribution of the paper. Four wind farm topologies were selected; radial, single-sided ring, double-sided ring and star topology. Four mitigation techniques were used for each topology: the pre-insertion resistor (PIR), the RC-snubber circuit, R-L smart choke and the surge capacitor. The simulations showed the failure of the VCB to open without any suppression measure. The addition of a surge capacitor didn't improve, while the remaining suppression measures were successful. It was noticed that PIR and R-L were optimal in radial and star topologies, which successfully reduced the SOV by an average of 52%. At the same time, R-C snubber was optimal for ring topologies that reduced SOV by an average of 70%. The presented results are not universally applicable to all wind farms, but they highlight the second contribution of the paper which is proving throught the presented investigation the dependence of the performance of SOV suppression measures upon the topology of the wind farm. The third contribution is presented in the conclusion that recommends for the selection of suppression measures in windfarms; simulations should be done to include the effect of the topology of the wind farm.

INDEX TERMS Wind farm topologies, switching overvoltage, vacuum circuit breaker, radial topology, single sided-topology, double sided topology, star topology, mitigation techniques, RC-snubber circuit.

NOMENCLATURE

A	: Manufacturer's parameter for the rate of rise of dielectric strength
B	: Breaker's TRV just before current zero
D	: High-frequency quenching capability of the vacuum circuit breaker just before contact separation
DSR	: Double sided ring
E	: Rate of rise of the high-frequency quenching capability
HFQC	: High-frequency quenching capability
I_{ch}	: Average chopping current
PIR	: Pre-Insertion Resistor
SSR	: Single sided ring
SOV	: Switching overvoltages
U	: Withstand voltage
VCB	: Vacuum circuit breaker

The associate editor coordinating the review of this manuscript and approving it for publication was Mouloud Denai.

I. INTRODUCTION

The transformation to renewable energy-based power sources has been accelerated by the continuous depletion of the reserve of fossil fuel and their negative impact on

TABLE 1. Summary of literature studying the impact of switching overvoltages in wind farms.

Ref.	Year	Studied SOV in wind farms	Studied different wind farm topologies	Suppression Measures							
				Control switching procedure	Surge Arrester	Shunt reactor	Cable length	Pre-Insertion Resistor (PIR)	RC-snubber	R-L choke	Surge capacitor
[3]	2021	✓	-	✓	-	-	-	-	-	-	-
[8]	2020	✓	-	-	✓	✓	-	-	-	-	-
[9, 10]	2021 2022	✓	-	-	✓	-	-	-	✓	✓	-
[11]	2022	✓	-	✓	✓	-	-	-	-	-	-
[12]	2021	✓	-	✓	-	-	✓	-	✓	-	-
[13]	2019	✓	-	-	-	-	-	-	-	-	-
[14]	2023	✓	-	-	-	-	-	✓	-	-	-
[15]	2020	✓	-	-	-	-	-	-	-	-	-
[16]	2019	✓	-	✓	-	-	-	-	-	-	-
[17]	2019	✓	-	-	-	-	-	-	-	-	-
[18]	2019	✓	-	-	-	-	-	-	-	-	-
[19, 20]	2014 2011	✓	✓	-	-	-	-	-	-	-	-
[21]	2012	✓	✓	-	-	-	-	-	-	-	-
[22]	2016	✓	-	-	-	-	-	-	-	-	✓
[23]	2015	✓	-	-	-	-	-	-	-	✓	-
[24]	2023	✓	-	-	-	-	-	-	✓	-	-
[25]	2022	✓	-	-	-	-	-	-	✓	-	-
[26]	2021	✓	-	-	-	-	-	-	✓	-	-
[27]	2016	✓	-	-	-	-	✓	-	-	-	-
[28]	2018	✓	-	-	✓	-	-	-	✓	-	-
[29]	2016	✓	-	-	✓	-	-	-	✓	-	-
[30]	2014	✓	-	-	✓	✓	-	✓	-	-	-
[31]	2018	✓	-	✓	-	-	-	-	-	-	-
[32]	2020	✓	-	-	✓	-	-	-	✓	-	-
[33]	2017	✓	-	-	✓	-	-	✓	-	-	-
[34]	2012	✓	-	-	✓	-	-	-	✓	-	-
[35]	2011	✓	-	-	-	-	-	-	-	-	-
[36]	2011	✓	-	-	-	-	-	-	-	-	-
[37]	2023	✓	-	✓	-	-	-	-	-	-	-

the environment. Wind power is considered to be one of the most widely used renewable energy sources. That expansion in the employment of wind farms has necessitated their adaptability to the surrounding environment through using various topologies for wind farms. An additional fator is also considered which is the degree of complexity of structure of wind farms. That is attributed to the requirement of specific environmental resources for their operation in addition to the usage a large number of various electrical components such as power transformers, underground cables and control algorithms [1]. The structure used to connect the wind turbines defines the topology of the wind farm. There are four basic topologies for wind farms, namely, Radial topology, Single-Sided Ring (SSR) topology, Double-Sided Ring (DSR) topology, and Star topology [2].

An intriguing problem in a wind farm operation is its continuous switching operation requirement as part of its control strategy. That results in multiple switching operations, which are subsequently associated with switching transient overvoltages that threaten the reliability of the wind farm [3], [4]. Hence, it has been the topic of study in multiple research to investigate the impact of switching overvoltages (SOV) on the insulation of the equipment of the system [5], [6], [7]. The main insights from the literature in this field of study for suppression measures in wind farms are presented in Table 1.

The table scans the various suppression measures for overvoltages used by researchers and shows the variance among researchers in selecting and analyzing mitigation techniques. The interesting point to be noticed is that most of the researchers considered a single topology in their studies, with few researchers that considered the impact of changing the topology of the wind farm on their results [19], [20]. This topic is very critical as the effectiveness of the selected mitigation technique depends on the type of wind farm topology in which it is utilized. For this reason, the main problem that this paper aims to address is to evaluate the impact of different topologies of the wind farm upon the performance of different mitigation techniques. In addition to the mitigation strategies presented in the table, active control schemes were used by researchers to control and mitigate overvoltages [38], [39], [40]. Even though these schemes are effective, they are not included in the paper as the main focus of this paper is to evaluate the performance of various mitigation measures with respect to different wind farm topologies. Thus, the contributions of this paper will be:

1) Analyze the impact of changing the wind farm topology upon SOV.

2) Investigating the effectiveness of mitigation techniques in terms of the wind farm topology where they are installed.
3) Presenting conclusions for the most suitable mitigation techniques for each wind farm topology.

The remaining sections of this paper are organized as follows. Section II presents the system under study. Section III presents the modeling of different elements within the system. The results from the simulations for each wind farm topology and different mitigation measures are presented in section IV. The results from section IV are further discussed and compared to the results from other works in section V. Finally, conclusions are drawn in section VI.

II. SYSTEM UNDER STUDY

The system understudy is based on a real wind farm in Zaafrana, Egypt. The system can generate up to 550 MW from 700 wind turbines that were assumed to have identical characteristics. Each turbine is rated at 1 MVA with a 690 V/22 kV transformer used for their connection. Cables are extended for a distance of 200-m between each two consecutive series turbines. A 220/22 kV substation connects the entire wind farm to the grid. The main features of the system will be fixed in all topologies while changing the connection between turbines according to the simulated topology. The topologies simulated will be radial, single-sided ring, double-sided ring and star connection, as shown in Figure 1. Feeder F1 is extended for 8 km in all topologies, while feeder F2 is set to 10.4 km in a single-sided ring topology and 6.5 km in a double-sided ring topology. Feeder F3 is extended to 1 km. For star topology, the length of the cables for each turbine will differ from other topologies, so for each turbine, the cable length will depend on its location. For example, cables for turbines W1 and W2 will be 200 m, while for turbines W3 and W4 will be 400 m. The modifications in [3] were reused in this paper. The modeling of each system component is discussed in the next section.

III. MODELING OF THE SYSTEM

A. MODELING OF THE VACUUM CIRCUIT BREAKER

Vacuum circuit breakers (VCBs) are widely used in switching wind farms because of their advantages of having lower maintenance requirements and longer operation life [11], [12], [13], [15], [17], [18], [24], [25], [26], [27], [28], [29], [32]. The VCB was modeled on ATP as a switch which was controlled using the MODELS component. The MODELS tool allows the control of the state of the switch as open or closed, which in turn, simulates the state of VCB either it had opened successfully and interrupted the arc or it had failed in opening. [41]. The MODELS tools are connected to measuring probes that measure the current flowing through the VCB and the voltage across it and use these measurements accordingly to define whether the VCB has interrupted the arc

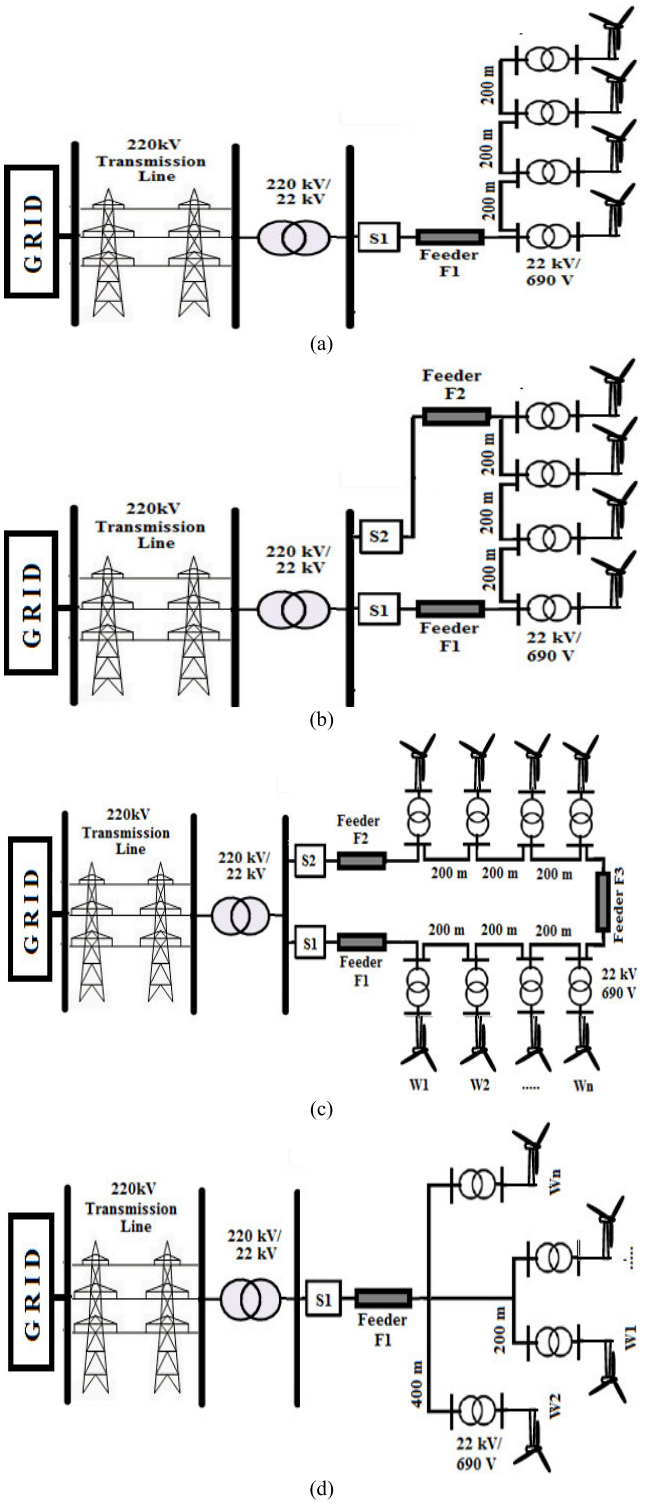

FIGURE 1. Topologies of the wind farm (a) Radial (b) Single sided ring (c) Double sided ring (d) Star.

or the arc has reignited, which is furtherly detailed in the given below sequence. The problem of arc reignition after its initial interruption is one of the main challenges that face the VCB. The reignations of the arc occur as a result of the increasing magnitude of SOVs that exceeds the withstand voltage of the

VCB. However, the VCB is still capable of re-interrupting the arc. That sequence of arc reignations and interruption is termed as multiple reignations of the arc. To consider this phenomenon within the VCB models, the following governing formulas are employed within the VCB model, which is presented in sequential order [42], [43]:

- The switch representing the state of the VCB will remain closed after the instant of the mechanical opening of the VCB to represent the presence of the arc.
- The VCB will successfully interrupt the arc for the first time when the current value flowing through the arc falls below the current chopping value. The average chopping current is shown in (1) [41].

$$\overline{I_{ch}} = (\omega \, \hat{\imath} \, \alpha \, \beta)^{q} \tag{1}$$

where $\omega = 2\pi(50\,\text{Hz})$, $\hat{\imath}$: amplitude of the 50 Hz current, $\alpha = 6.2\times10^{-16}$ sec, $\beta = 14.3q = (1-\beta)^{-1}$.

- The successful interruption of the arc would lead to the initialization of transient recovery voltage (TRV) across the contacts of the VCB. When the TRV becomes greater than the withstand voltage of the VCB, which is calculated from (2), the switch recloses, simulating the reignitions of the arc.

$$U = A\left(t - t_{open}\right) + B \tag{2}$$

where U: the withstand voltage, t_{open}: the moment of contact separation, A: Manufacturer's parameter for rate of rise of dielectric strength taken as 2 V/μs [41], B: Breaker's TRV just before current zero and in this study B was considered as zero [41].

- After the reignition of the arc, the VCB could re-interrupt the arc when high-frequency quenching capability (HFQC) exceeds the current rate of change at zero crossing and the switch is reopened. The HFQC is given in (3)

$$HFQC = E\left(t - t_{open}\right) + D \tag{3}$$

where E: Rate of rise of the HFQC of the VCB and E is considered as 600 A/μs^2 [41], D: is HFQC of the VCB just before contact separation and D is considered zero in this study [41].

The previous sequence is shown as a flow chart in figure 2. Finally, the VCB model was validated by using the test circuit provided in [44].

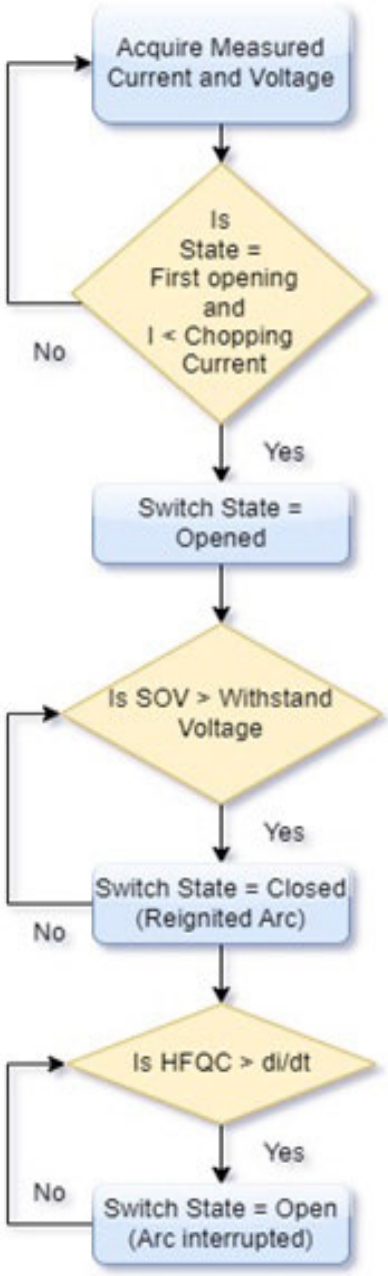

FIGURE 2. Flowchart of VCB Model.

B. TRANSMISSION LINES, FEEDERS AND CABLES

Transmission lines were modeled by their respective frequency-dependent transmission line model. The parameters employed in modeling of transmission lines are given Table 2. The frequency-dependent cable model was used to model cables. The lengths of cable depends on their location such that cables for turbines W1 and W2 are 200 m in length, while for turbines W3 and W4, cables are 400 m in length.

TABLE 2. Transmission line parameters.

	Positive and negative sequence parameters	Zero sequence parameters
Resistance (Ω/km)	0.03	0.13
Reactance (Ω/km)	0.306	0.83
Susceptance (mS/km)	3.25	2.3

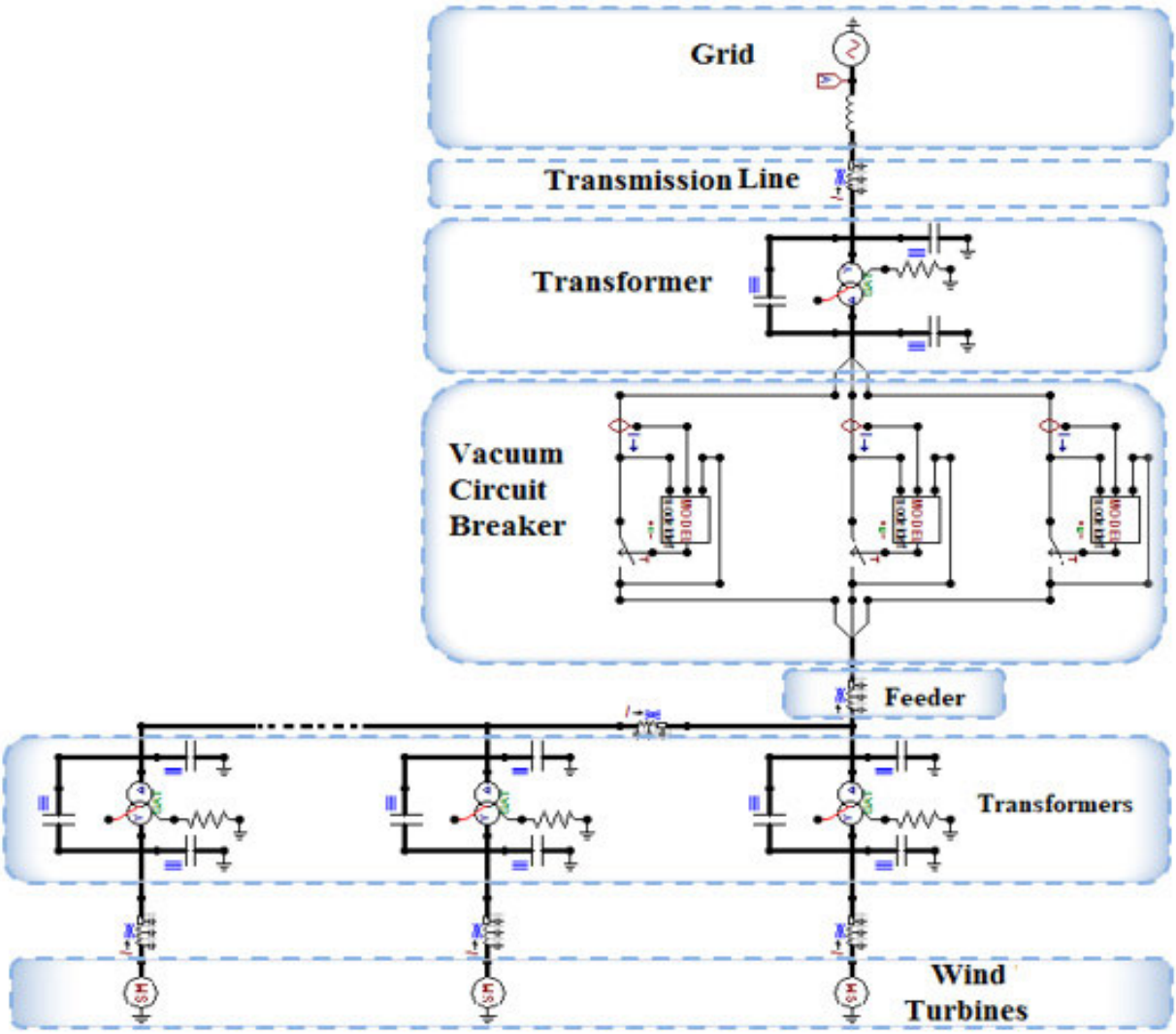

FIGURE 3. Schemetaic diagram for the modeled systems using ATP software with turbines connected in radial topology.

C. POWER TRANSFORMERS

The modeling of the transformer included the utilization of the frequency-dependent transformer component available on ATP, which is set to 690V/22 kV to connect the generators of the wind turbines to the farm. For the sake of accurate transformer modeling, stray capacitances are also considered as shown in figure 3. Stray capacitances are considered between each transformer winding, high voltage HV and low voltage LV and the ground and such capacitances are termed as C_HV_GNG and C_LV_GND. Also, the mutual capacitance between the phase of the two windings of the main transformers is considered. [3], [45]. The parameter values of the stray capacitances were selected from the typical values given in [10]. The approximate values employed in this study were in the range of a few nano-farads of 1 to 3 nF as employed in [10].

D. WIND TURBINE

The main element within the turbine is the generator, which is modeled using type 59 synchronous machine component available on ATP/EMTP. The generator parameters were selected based on the system description provided in the previous section. The operating voltage of generators is 690 V. The leakage reactance of the generator is 0.1 H [45]. Each generator is connected to the farm through a 690V/22 kV transformer, modeled as mentioned in the previous subsection.

The modeling schematic as generated by the ATP software package is shown in figure 3. The schematic shows the VCB model using MODELS tool, the transformer with connected stray capacitance, the grid, transmission lines and wind turbines connected in radial topolog. For the remaining topologies, the same schematic is used with the connection of the turbines restructured as in figue 1.

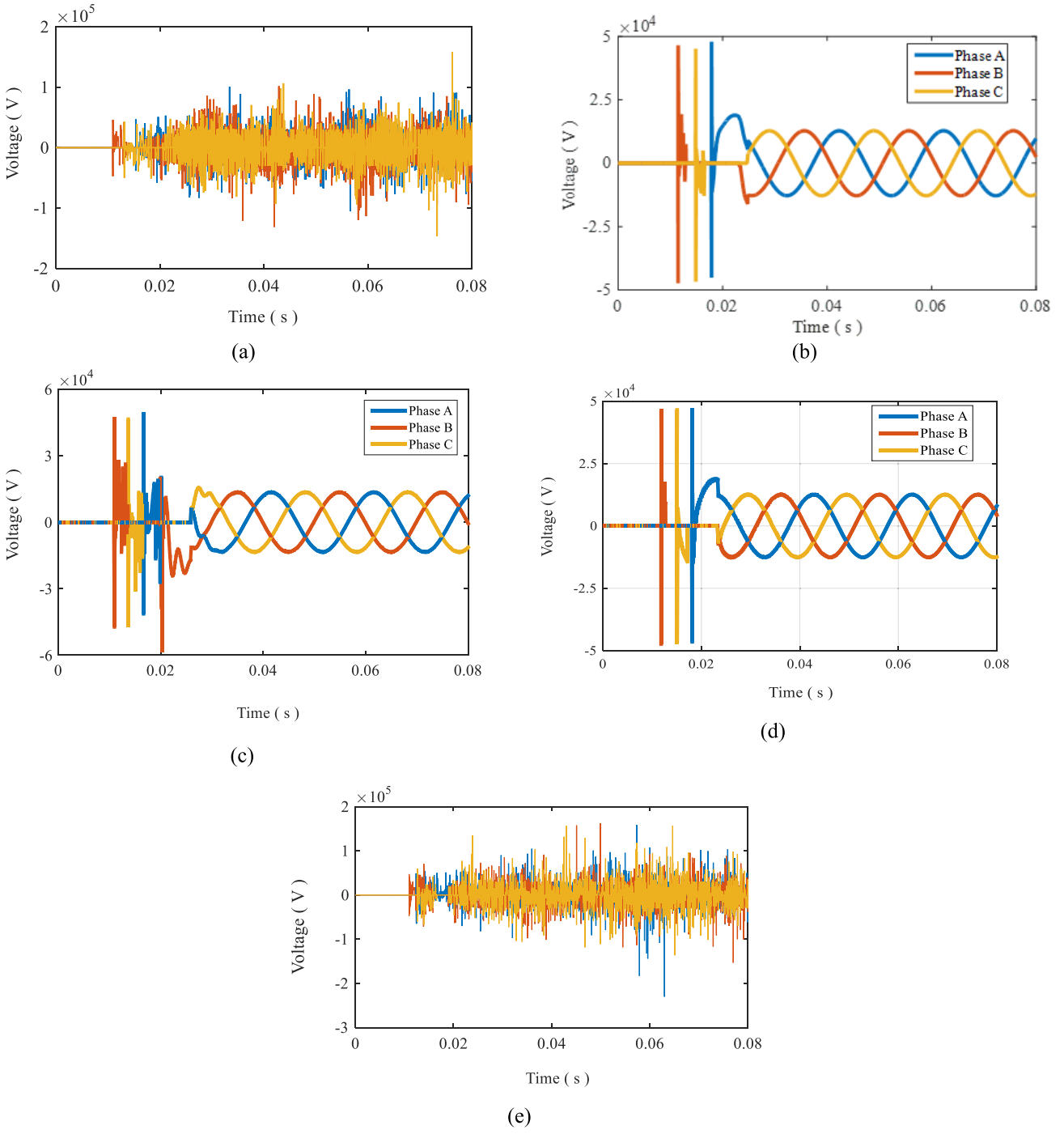

FIGURE 4. SOV across VCB S1 in radial topology (a) Without mitigation (b) With PIR (c) with R-C snubber circuit (d) with R-L smart choke (e) with surge capacitor.

IV. SIMULATION RESULTS

The sequence of the simulation process included running simulation test without using any mitigation measure for the selected topology. Secondly, mitigation techniques were used were used each one at a time for the selected topology. Finally, the previous steps were repeated for other topologies. This sequence would allow the evaluation of the capability of each mitigation technique in suppressing SOV for each topology. Also, it would allow comparing the degree of effectivity of a specific mitigation measure in different topologies. Simulations were undergone using ATP/EMTP simulation platform. The mitigation techniques studied include four schemes; RC snubber [8], [9], [10], [11], pre-insertion resistor (PIR) [14] and surge capacitor [22]. The parameters of each scheme (R and/or C) were set based on the ranges of the recommended values from the literature [41]. The values of R and L

of the smart choke coil were based on the recommendations of [46]. The ranges for the parameters of mitigation methods were tested and the values that gave an optimum reduction in SOV were selected. The selected values were 100 Ω for the PIR, R = 100 and C = 1 μF for the RC snubber circuit, the capacitance of the surge capacitor was 1 μF, R = 50 Ω, 1.5 mH for the smart choke inductor. The simulation results for each topology are presented in the following subsections. Another mitigation technique is a fault current limiter (FCL) which is used mainly to limit the current flowing through the systems during faults and consequently reduce the following transient recovery voltage [47]. However, this paper focuses on switching overvoltages in non-faulty cases, so this paper will not consider this scheme.

A. SIMULATION RESULTS FOR RADIAL TOPOLOGY

The VCB named S1 in the radial topology shown in Figure 1(a) was first tested for opening without any additional mitigation measures. The results showed the VCB had failed for the selected A, B, E and D parameters. Such failure could be overcome by upgrading the VCB to have higher A, B, E and D parameters. Another path to solve this problem is by integrating the VCB with one of the previously mentioned mitigation techniques. The results showed that with the addition of suitable mitigation measures, the VCB had opened successfully except for the surge capacitor, which remained insuccesfull in arc interruption. The results showed the peak of the recorded SOV for each mitigation technique which are presented in Table 3. The results are shown in Figure 4.

TABLE 3. Peak value of switching overvoltage across VCB S1 in radial topology.

Mitigation Method	Switching Overvoltage (kV)		
	Phase A	Phase B	Phase C
Without mitigation		Fail	
With PIR	47.315	47.841	46.973
With R-C	57.831	48.804	46.586
With choke coil R-L	47.375	46.500	46.777
With surge capacitor		Fail	

B. SIMULATION RESULTS FOR SINGLE-SIDED RING TOPOLOGY

The same sequence earlier used for radial topology has been re-applied for single-sided topology. The results show

TABLE 4. Peak value of SOV across VCB S1 in Single-sided ring topology.

Mitigation Method	Switching Overvoltage (kV)		
	Phase A	Phase B	Phase C
Without mitigation		Fail	
With PIR	47.197	47.205	13.531
With R-C	26.037	46.870	34.270
With choke coil R-L	47.239	47.202	14.226
With surge capacitor		Fail	

TABLE 5. Peak value of SOV across VCB S1 in a double-sided ring topology.

Mitigation Method	Switching Overvoltage (kV)		
	Phase A	Phase B	Phase C
Without mitigation		Fail	
With PIR	47.115	46.512	33.241
With R-C	27.399	46.501	17.038
With choke coil R-L	46.537	46.130	11.926
With surge capacitor		Fail	

TABLE 6. Peak value of SOV across VCB S1 in a star topology.

Mitigation Method	Switching Overvoltage (kV)		
	Phase A	Phase B	Phase C
Without mitigation		Fail	
With PIR	47.301	47.618	46.888
With R-C	68.466	74.587	46.776
With choke coil R-L	47.267	49.264	46.649
With surge capacitor		Fail	

TABLE 7. Percentage of reduction of SOV for different mitigation measures in different wind farm topologies.

Wind Farm Topology	Radial	SSR	DSR	Star
Mitigation Technique	Percentage of Reduction in SOV of phase A			
PIR	52.685	52.803	52.885	52.699
RC Snubber	42.169	73.963	72.601	31.534
R-L Choke	52.625	52.761	53.463	52.733
	Percentage of Reduction in SOV of phase B			
PIR	52.159	52.795	53.488	52.382
RC Snubber	51.196	53.13	53.499	25.413
R-L Choke	53.5	52.798	53.87	50.736
	Percentage of Reduction in SOV of phase C			
PIR	53.027	86.469	66.759	53.112
RC Snubber	53.414	65.73	82.962	53.224
R-L Choke	53.223	85.774	88.074	53.351

TABLE 8. Comparative evaluation of the reduction in overvoltage in this paper and literature.

Refernece	[10]	[14]	[24]	[25]	[26]	This Paper	
Studied Wind farm topology	Radial	Radial	Radial	Star	DSR	Radial Satr	SSR DSR
	Percentage of Reduction in SOV						
PIR	-	79.4	-	-	-	52	60.1
RC Snubber	37.9	-	73.2	23	60.5	42.5	70
R-L Choke	14.7	66.3	-	-	-	52	63.5

the failure in two cases; VCB opening without mitigation techniques and with surge capacitor. Other mitigation measures opened successfully, as presented in Table 4 and Figure 5.

C. SIMULATION RESULTS FOR DOUBLE-SIDED RING TOPOLOGY

The double-sided ring topology is tested in the same manner as in previous cases with its results presented in table 5 and shown in figure 6.

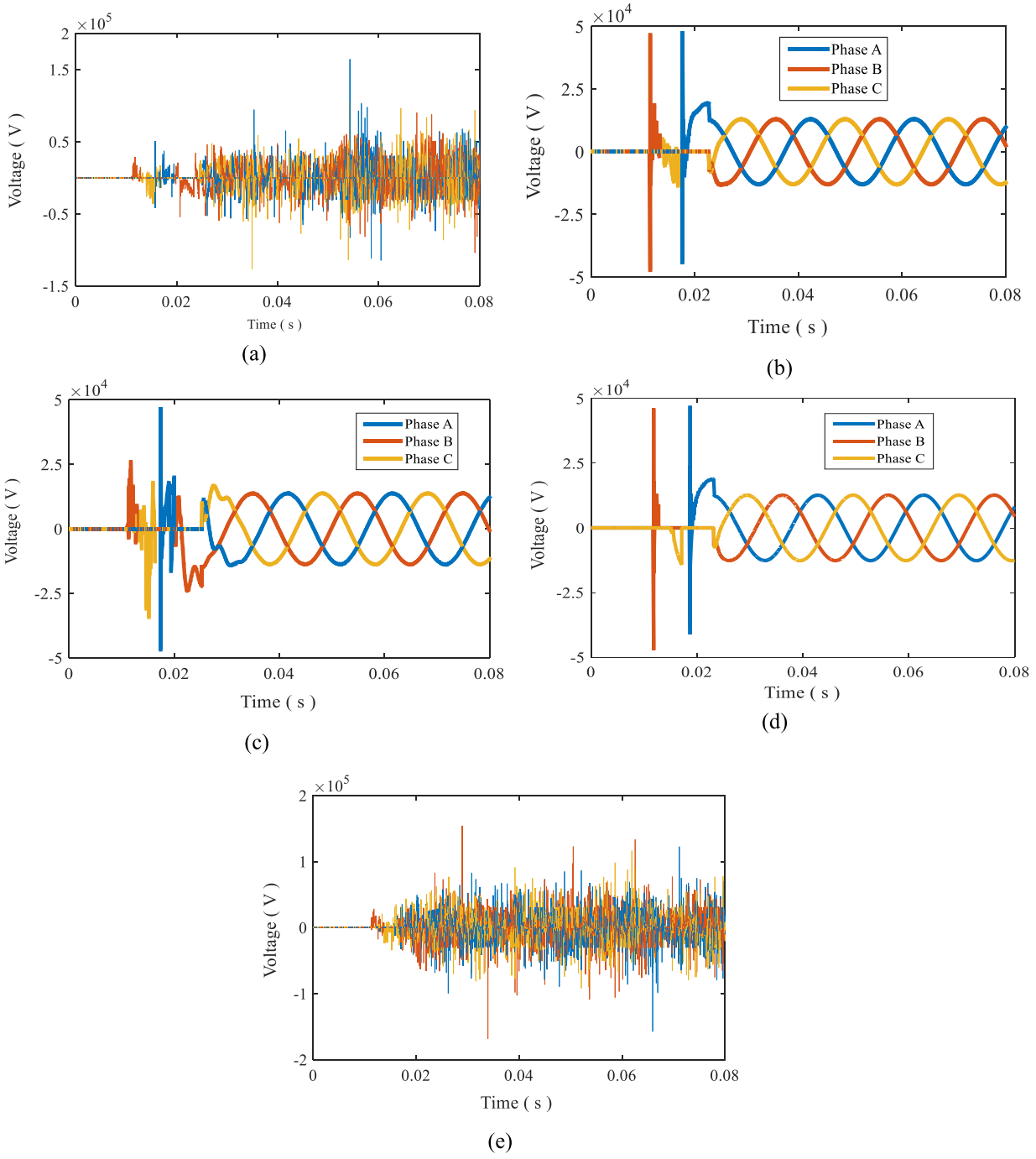

FIGURE 5. SOV across VCB S1 in SSR topology (a) Without mitigation (b) With PIR (c) with R-C snubber circuit (d) with R-L smart choke (e) with surge capacitor.

D. SIMULATION RESULTS FOR STAR TOPOLOGY

The final topology to be tested is the star topology. The results for this topology are presented in Table 6 and shown in Figure 7.

V. ANALYSIS AND DISCUSSION

The simulation results in all four topologies of wind farms showed the success of three mitigation measures in suppressing the SOV: the PIR, RC-snubber circuit and R-L smart coke. The values of the reduced SOV in each topology will be compared to analyze these results. The results of Tables 3 to 6 will be used to calculate the percentage of reduction in SOV between each mitigation measure and the SOV generated when no mitigation was used. The percentage of reduction of SOV is presented in Table 7 and is graphically interpreted in Figure 8. From the results shown, it could be concluded that for radial and star topologies, both PIR and R-L smart choke were

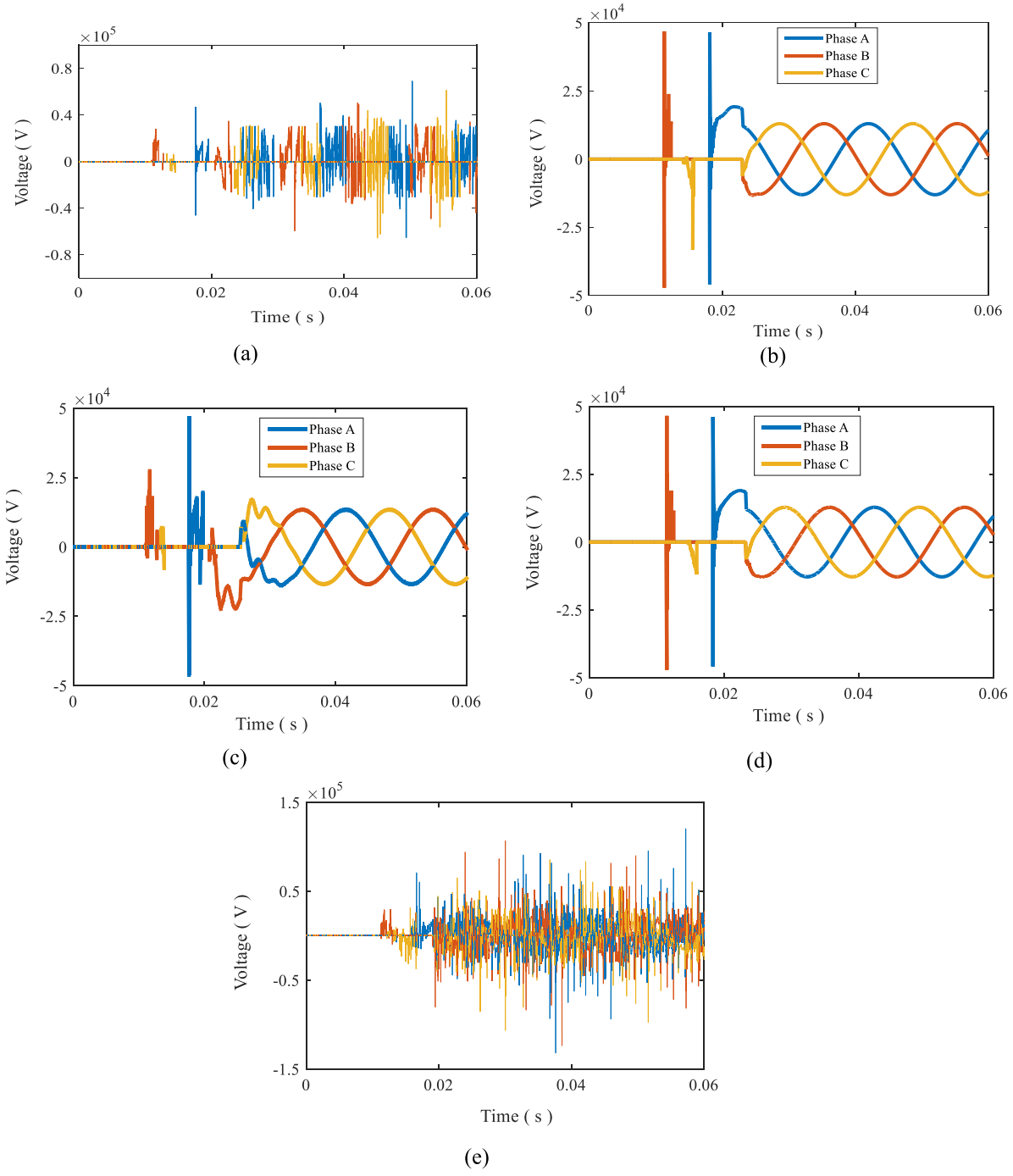

FIGURE 6. SOV across VCB S1 in DSR topology (a) Without mitigation (b) With PIR (c) with R-C snubber circuit (d) with R-L smart choke (e) with surge capacitor.

the most effective and capable of reducing the SOV by an average of 52 %. While for single-sided star (SSR) and double-sided ring topologies, RC-snubber was the most effective technique, with an average reduction of 70 %. A second aspect of analysis could be seen from the point of view of each mitigation measure to show how changing the topology of the wind farm affects their capability in suppressing the SOV. The percentage of reduction in phase A for PIR, RC and R-L mitigation measures for all topologies are shown in Figure 8 (a). Figures 8 (b) and (c) show the same aspect for phases B and C. It could be seen from Figure 8(a) and (b) that the effectivity of RC in reducing the SOV was maximized for both single and double-sided ring circuits. Figure 8 also shows that the PIR and R-L mitigation techniques were equally effective in all cases, maximizing their effectiveness in radial and star topology. The reason for having different levels of effectiveness for different techniques in each topology could be explained as

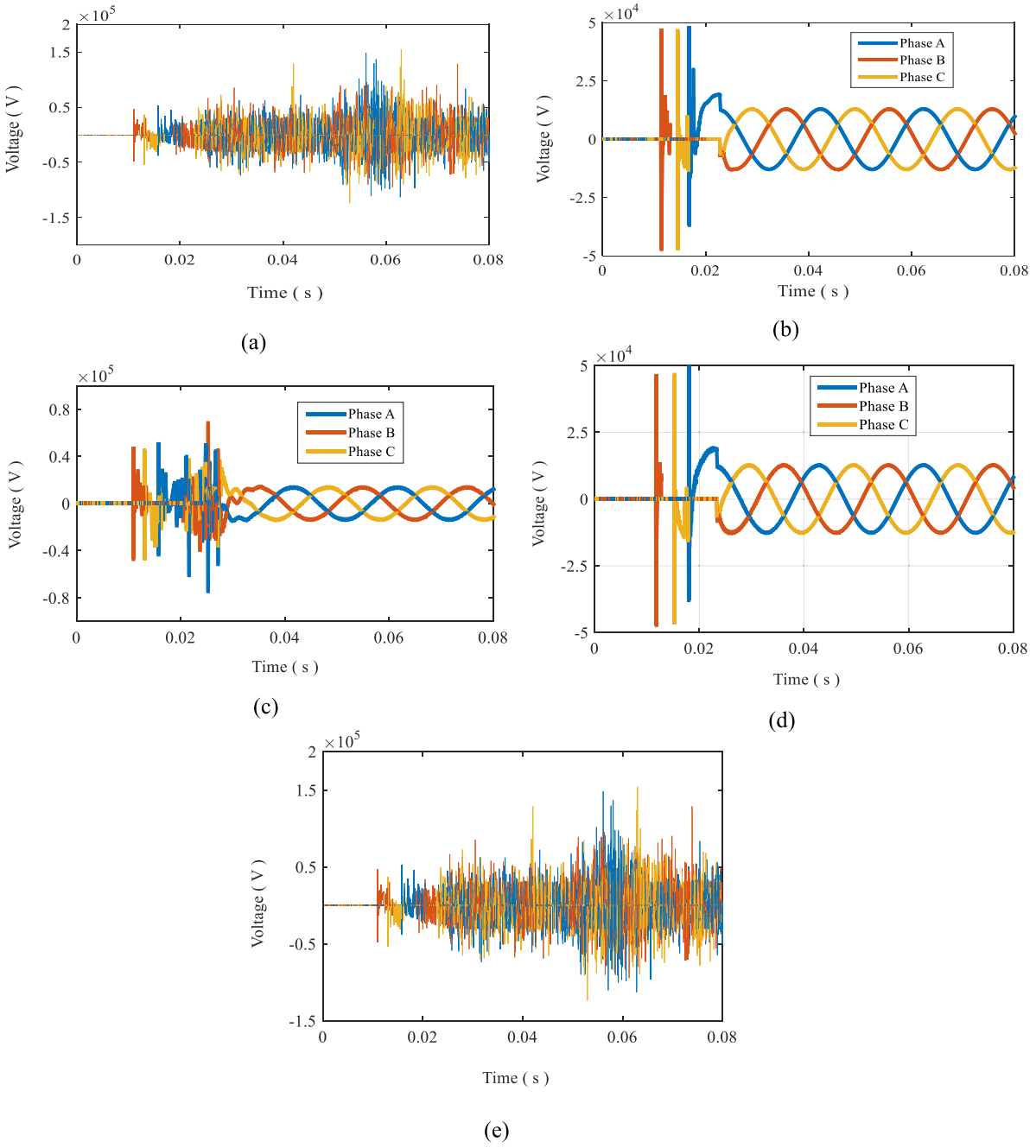

FIGURE 7. SOV across VCB S1 in a star topology (a) Without mitigation (b) With PIR (c) with R-C snubber circuit (d) with R-L smart choke (e) with surge capacitor.

follows. For PIR and R-L techniques, their effectiveness are considered relatively unchanged in all topologies as shown in Fig. 8 (a) as their elements (R and L) have nearly the same effect in all topologies. While for R-C circuits, their effectiveness is maximized in single sided and double sided ring topologies (as shown in Fig. 8(a)). That increased effectivenss depends on the ability of the capacitive element of the R-C circuit in mitigating the SOV under the voltage distribution in ring topologies. As for ring topologies wind turbines are connected from both sides to the grid allowing a reduced voltage drop through cables. Such a condition is not present in star and radial topologies and hence, the R-C effectiveness in these two previous topologies are considered lower than PIR and R-L techniques.

To further evaluate the presented results, they were compared to the results presented from other works on the same topic. The results are presented in Table 8. The results show that other works did not cover the impact of different suppression measures for various wind farm topologies but were limited to specific topologies. The results also show that the selected suppression measures are generally effective, as concluded by the paper. However, the level of impact of a specific

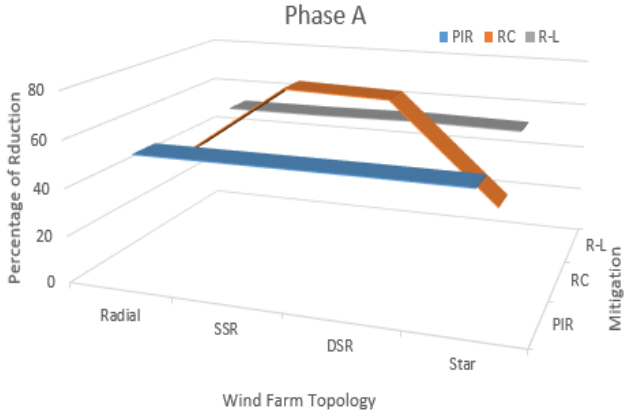

(a)

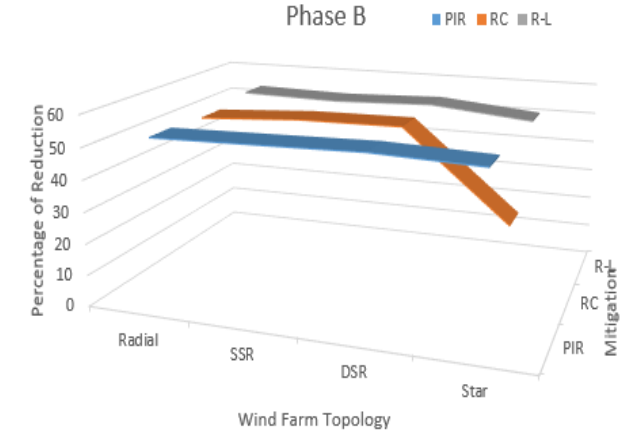

(b)

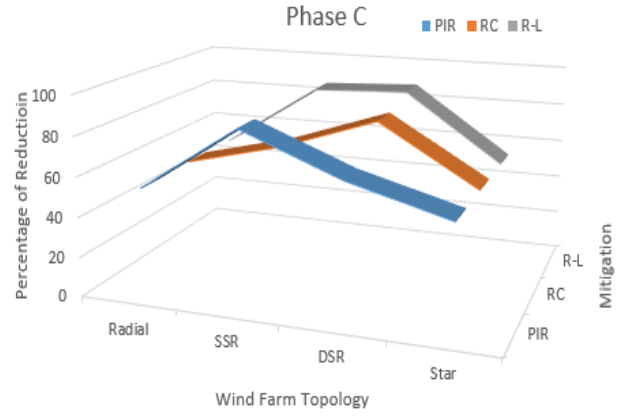

(c)

FIGURE 8. Percentage of reduction in SOV with different mitigation techniques in different wind farm topologies for (a) Phase A (b) Phase B (c) Phase C.

suppression measure within a specific wind farm topology varies between different references as presented in the table. This is attributed to the different parameters affecting the final outcome, including the length of the feeders and VCB parameters. Hence, it could be concluded that the presented results can not be generalized for all wind farms but proves that the effectiveness of different suppression measures are affected by the change in the wind farm topology. That point should be considered when selecting the appropriate suppression measure for a specific wind farm topology.

VI. CONCLUSION

The impact of different wind farm topologies on different mitigation techniques was investigated. To perform this investigation, a real wind farm system located in Zaafrana, Egypt, was modeled using ATP/EMTP software. The basic structure of the farm was modified to four wind farm topologies; radial, single-sided ring, double-sided ring and star topology. In each topology, four suppression techniques for switching overvaoltages were used in one by one order to define their effectiveness in reducing the overvoltage. These suppression measures include the pre-insertion resistor (PIR), the RC-snubber circuit, R-L smart choke and the surge capacitor. The simulation tests were undergone for each topology, and each suppression measure was used within each topology. The switching overvoltage (SOV) was recorded in each case to evaluate the amount of reduction the suppression measure had induced in SOV. The results showed the failure of VCB to open independently without any mitigation measure. The usage of surge capacitor did not overcome the problem but for the remaining mitigation measures, the VCB opened successfully. The results confirmed the dependence of the amount of reduction in SOV by suppression measure upon the type of the wind farm topology. The optimum degree of reduction in SOV for each topology could be summarized as follows:

1) For radial topology, the PIR and R-L smart choke were the most effective, reaching a 52 % average reduction.
2) The RC-snubber was the most effective technique for both single and double-sided ring topologies, with an average reduction of 70 %.
3) For star topology, the PIR and R-L smart choke were the most effective, reaching a 52 % average reduction.

Based on these results, it could be concluded that the degree of suitability of a certain overvoltage suppression measure is dependent upon the type of wind farm topology. Therefore, It is recommended that design engineers should perform a simulation study to select the optimal mitigation technique that is suited for the selected wind farm topology.

ACKNOWLEDGMENT

The authors would like to acknowledge Deanship of Scientific Research, Taif University for funding this work.

REFERENCES

[1] J. F. Manwell, J. G. McGowan, and A. L. Rogers, *Wind Energy Explained: Theory, Design and Application*. Hoboken, NJ, USA: Wiley, 2010.
[2] A. Holdyk, J. Holbøll, E. Koldby, and A. Jensen, "Influence of offshore wind farms layout on electrical resonances," in *Proc. Cigre Session*, Paris, France, 2014, p. C4-310_2014.
[3] M. Elshahed, A. Ragab, M. Gilany, and M. Sayed, "Investigation of switching over-voltages with different wind farm topologies," *Ain Shams Eng. J.*, vol. 12, no. 3, pp. 2695–2707, Sep. 2021.
[4] W. Sweet, "Danish wind turbines take unfortunate turn," *IEEE Spectr.*, vol. 41, no. 11, pp. 30–34, Nov. 2004.

[5] T. Abdulahovic, "Analysis of high frequency electrical transients in offshore wind parks," M.S. thesis, Dept. Energy Environ., Chalmers Univ. Technol., Sweden, 2009.
[6] L. Liljestrand, A. Sannino, H. Breder, and S. Thorburn, "Transients in collection grids of large offshore wind parks," *Wind Energy*, vol. 11, no. 1, pp. 45–61, Jan. 2008.
[7] T. Abdulahovic and T. Thiringer, "Voltage stress in a transformer winding during very fast transients caused by breaker closing event," *IEEE Trans. Power Del.*, vol. 29, no. 4, pp. 1946–1954, Aug. 2014.
[8] A. Akinrinde, A. Swanson, and I. Davidson, "Investigation and mitigation of temporary overvoltage caused by de-energization on an offshore wind farm," *Energies*, vol. 13, no. 17, p. 4439, Aug. 2020.
[9] Y. Xin, B. Zhao, Q. Liang, J. Zhou, T. Qian, Z. Yu, and W. Tang, "Development of improved suppression measures against reignition overvoltages caused by vacuum circuit breakers in offshore wind farms," *IEEE Trans. Power Del.*, vol. 37, no. 1, pp. 517–527, Feb. 2022.
[10] Y. L. Xin, Y. H. Yang, B. N. Zhao, L. Xu, Z. Y. Yu, and W. H. Tang, "Configuration of suppression schemes against high-frequency transient reignition overvoltages caused by shunt reactor switching-off in offshore wind farms," *Int. J. Electr. Power Energy Syst.*, vol. 141, Oct. 2022, Art. no. 108170.
[11] Q. Sun, Z. Zheng, L. Huang, F. Wang, L. Zhong, and S. Chen, "Investigation on reignition probability of switching overvoltage caused by vacuum circuit breaker in offshore wind farms," *IEEE Trans. Power Del.*, vol. 37, no. 5, pp. 4438–4447, Oct. 2022.
[12] Y. Geng, J. Dong, X. Chen, L. Zhang, J. Yan, Y. Geng, J. Peng, and K. Wang, "Three-phase modeling of 40.5-kV vacuum circuit breaker switching off shunt reactors and overvoltage suppression measure analysis," *Electr. Power Syst. Res.*, vol. 194, May 2021, Art. no. 107058.
[13] J. Zhou, Y. Xin, W. Tang, G. Liu, and Q. Wu, "Impact factor identification for switching overvoltage in an offshore wind farm by analyzing multiple ignition transients," *IEEE Access*, vol. 7, pp. 64651–64662, 2019.
[14] A. Said, M. Ezzat, M. A. Abd-Allah, M. M. Fouda, and M. A. Abouelatta, "Optimization-based mitigation techniques of the temporary overvoltage in large offshore wind farm," *IEEE Access*, vol. 11, pp. 6320–6330, 2023.
[15] S. Ghasemi, M. Allahbakhshi, B. Behdani, M. Tajdinian, and M. Popov, "Probabilistic analysis of switching transients due to vacuum circuit breaker operation on wind turbine step-up transformers," *Electr. Power Syst. Res.*, vol. 182, May 2020, Art. no. 106204.
[16] Y. Li, J. Guo, Z. Xi, S. Wang, S. Ma, B. Zhao, G. Wu, and T. Wang, "Over-voltage suppression methods for the MMC-VSC-HVDC wind farm integration system," *IEEE Trans. Circuits Syst. II, Exp. Briefs*, vol. 67, no. 2, pp. 355–359, Feb. 2020.
[17] N. A. Kafshgari, N. Ramezani, and H. Nouri, "Effects of high frequency modeling & grounding system parameters on transient recovery voltage across vacuum circuit breakers for capacitor switching in wind power plants," *Int. J. Electr. Power Energy Syst.*, vol. 104, pp. 159–168, Jan. 2019.
[18] Y. L. Xin, W. H. Tang, J. J. Zhou, Y. H. Yang, and G. Liu, "Sensitivity analysis of reignition overvoltage for vacuum circuit breaker in offshore wind farm using experiment-based modeling," *Electr. Power Syst. Res.*, vol. 172, pp. 86–95, Jul. 2019.
[19] T. Zhang, L. Sun, and Y. Zhang, "Study on switching overvoltage in offshore wind farms," *IEEE Trans. Appl. Supercond.*, vol. 24, no. 5, pp. 1–5, Oct. 2014.
[20] F. Villar, M. Reza, K. Srivastava, and S. L. Da, "High frequency transients propagation and the multiple reflections effect in collection grids for offshore wind parks," in *Proc. IEEE Power Energy Soc. General Meeting*, Detroit, MI, USA, Jul. 2011, pp. 1–7.
[21] A. Chennamadhavuni, K. K. Munji, and R. Bhimasingu, "Investigation of transient and temporary overvoltages in a wind farm," in *Proc. IEEE Int. Conf. Power Syst. Technol. (POWERCON)*. Auckland, New Zealand: IEEE, 2012, pp. 1–6.
[22] Y. Xin, B. Liu, W. Tang, and Q. Wu, "Modeling and mitigation for high frequency switching transients due to energization in offshore wind farms," *Energies*, vol. 9, no. 12, p. 1044, Dec. 2016.
[23] D. Smugala, W. Piasecki, M. Ostrogorska, M. Florkowski, M. Fulczyk, and O. Granhaug, "Wind turbine transformers protection method against high-frequency transients," *IEEE Trans. Power Del.*, vol. 30, no. 2, pp. 853–860, Apr. 2015.
[24] Z. Pu, H. Liu, Y. Wang, X. Yu, and T. Wu, "Simulation and protection of reignition overvoltage in wind farm considering microscopic dielectric recovery process of vacuum circuit breaker," *Energies*, vol. 16, no. 4, p. 2070, Feb. 2023.
[25] Z. Zheng, Q. Sun, J. Yang, S. Chen, F. Wang, and L. Zhong, "Investigation on overvoltage caused by vacuum circuit breaker switching off shunt reactor in offshore wind farms," *High Voltage*, vol. 7, no. 5, pp. 936–949, Oct. 2022.
[26] J. Tao, Q. Yang, X. Zheng, Y. He, R. Wang, H. Lv, and J. Zhang, "Switching transients caused by vacuum circuit breakers in collection grids of offshore wind farms," *Wind Energy*, vol. 24, no. 12, pp. 1501–1516, Dec. 2021.
[27] S. M. Ghafourian, I. Arana, J. Holbøll, T. Sørensen, M. Popov, and V. Terzija, "General analysis of vacuum circuit breaker switching overvoltages in offshore wind farms," *IEEE Trans. Power Del.*, vol. 31, no. 5, pp. 2351–2359, Oct. 2016.
[28] J. Zhou, W. Tang, Y. Xin, and Q. Wu, "Investigation on switching overvoltage in an offshore wind farm and its mitigation methods based on laboratory experiments," in *Proc. IEEE PES Asia–Pacific Power Energy Eng. Conf. (APPEEC)*, Oct. 2018, pp. 189–193.
[29] Q. Zhou, Y. Cheng, X. Bian, F. Liu, and Y. Zhao, "Analysis of restrike overvoltage of circuit breakers in offshore wind farms," *IEEE Trans. Appl. Supercond.*, vol. 26, no. 7, pp. 1–5, Oct. 2016.
[30] E. Awad and E. B. F. Youssef, "Mitigation of switching overvoltages due to energization procedures in grid-connected offshore wind farms," *Int. J. Adv. Res. Electr., Electron. Instrum. Eng.*, vol. 3, no. 1, pp. 7020–7028, 2014.
[31] G. Liu, Y. Guo, Y. Xin, L. You, X. Jiang, M. Zheng, and W. Tang, "Analysis of switching transients during energization in large offshore wind farms," *Energies*, vol. 11, no. 2, p. 470, Feb. 2018.
[32] Y. Guo, X. Jiang, Y. Chen, M. Zheng, G. Liu, X. Li, and W. Tang, "Reignition overvoltages induced by vacuum circuit breakers and its suppression in offshore wind farms," *Int. J. Electr. Power Energy Syst.*, vol. 122, Nov. 2020, Art. no. 106227.
[33] A. Akinrinde, A. Swanson, and R. Tiako, "Investigation and analysis of temporary overvoltages caused by filter banks at onshore wind farm substation," *Int. J. Renew. Energy Res.*, vol. 7, no. 2, pp. 770–777, 2022.
[34] A. H. Soloot, H. K. Høidalen, and B. Gustavsen, "The assessment of overvoltage protection within energization of offshore wind farms," *Energy Procedia*, vol. 24, pp. 151–158, Jan. 2012.
[35] A. Soloot, H. K. Hoidalen, and B. Gustavsen, "A study of switching overvoltages in offshore wind farm," in *Proc. 17th Int. Symp. High Voltage Eng.*, 2011.
[36] R. King, F. Moore, N. Jenkins, A. Haddad, H. Griffiths, and M. Osborne, "Switching transients in offshore wind farms-impact on the offshore and onshore networks," in *Proc. Int. Conf. Power Syst. Transients*. Delft, The Netherlands: IPST, 2011. [Online]. Available: https://www.ipstconf.org/papers/Proc_IPST2011/11IPST039.pdf
[37] Q. Sun, Z. Zheng, J. Zhang, X. Li, F. Wang, S. Chen, and L. Zhong, "Investigation on multiple reignitions caused by vacuum circuit breaker switching off shunt reactor considering contact travel in offshore wind farms," *IEEE Trans. Power Del.*, early access, Feb. 1, 2023. [Online]. Available: https://ieeexplore.ieee.org/abstract/document/10034842
[38] G. C. Kryonidis, E. O. Kontis, A. I. Chrysochos, C. S. Demoulias, and G. K. Papagiannis, "A coordinated droop control strategy for overvoltage mitigation in active distribution networks," *IEEE Trans. Smart Grid*, vol. 9, no. 5, pp. 5260–5270, Sep. 2018.
[39] T. L. Vandoorn, J. De Kooning, B. Meersman, and L. Vandevelde, "Voltage-based droop control of renewables to avoid on–off oscillations caused by overvoltages," *IEEE Trans. Power Del.*, vol. 28, no. 2, pp. 845–854, Apr. 2013.
[40] G. C. Kryonidis, C. S. Demoulias, and G. K. Papagiannis, "A new voltage control scheme for active medium-voltage (MV) networks," *Electr. Power Syst. Res.*, vol. 169, pp. 53–64, Apr. 2019.
[41] M. A. Ebrahim, T. Elyan, F. Wadie, and M. A. Abd-Allah, "Optimal design of RC snubber circuit for mitigating transient overvoltage on VCB via hybrid FFT/Wavelet genetic approach," *Electr. Power Syst. Res.*, vol. 143, pp. 451–461, Feb. 2017.
[42] C. Collet and B. De Metz-Noblat, "Vacuum circuit breaker model: Application case to motors switching," in *Proc. Int. Conf. Power Syst. Transients*, Lyon, France, Jun. 2007. [Online]. Available: https://www.ipstconf.org/papers/Proc_IPST2007/07IPST106.pdf
[43] J. Helmer and M. Lindmayer, "Mathematical modeling of the high frequency behavior of vacuum interrupters and comparison with measured transients in power systems," in *Proc. 17th Int. Symp. Discharges Electr. Insul. Vac.*, Berkeley, CA, USA, 1996, pp. 323–331.

[44] H. Xue and M. Popov, "Analysis of switching transient overvoltages in the power system of floating production storage and offloading vessel," *Electr. Power Syst. Res.*, vol. 115, pp. 3–10, Oct. 2014.
[45] M. A. Abouelatta, M. Ezzat, M. A. Abd-Allah, and A. Said, "Analysis and mitigation of the lightning overvoltage in capacitively coupling grid connected offshore wind turbine," *Int. J. Electr. Eng. Informat.*, vol. 14, no. 2, pp. 443–464, Jun. 2022.
[46] D. Smugała, W. Piasecki, M. Ostrogórska, M. Florkowski, M. Fulczyk, and O. Granhaug, "New approach to protecting transformers against high frequency transients–wind turbine case study," *Prz. Elektrotech.*, no. 89, pp. 186–190, 2013.
[47] Q. Tang, S. Jia, Y. Zhang, S. Xiu, W. Mo, Y. Wang, and H. Su, "Analysis influence a novel inductive fault current limiter circuit breaker 500 kV power system," *High Voltage*, vol. 6, no. 6, pp. 997–1008, 2021.

TAMER ELIYAN was born in Qaluobia, Egypt, in September 1983. He received the B.Sc. degree (Hons.) in electrical power and machines, and the M.Sc. and Ph.D. degrees in high voltage engineering from the Electrical Power and Machines Department, Faculty of Engineering at Shoubra, Benha University, Cairo, Egypt, in 2005, 2010, and 2015, respectively. He is currently an Associate Professor with the Electrical Engineering Department, Faculty of Engineering at Shoubra, Benha University. His research interests include transient phenomena in power networks and power systems, renewable energy, high voltage materials engineering, high voltage circuit breakers, and smart grid.

IBRAHIM B. M. TAHA received the B.Sc. degree from the Faculty of Engineering at Tanta, Tanta University, Egypt, in 1995, the M.Sc. degree from the Faculty of Engineering at Mansoura, Mansoura University, Egypt, in 1999, and the Ph.D. degree in electrical power and machines from the Faculty of Engineering, Tanta University, in 2007. Since 1996, he has been a Teaching Staff with the Faculty of Engineering, Tanta University. He is currently an Assistant Professor with the Electrical Engineering Department, Taif University, Saudi Arabia. He is also a Professor with the Electrical Power and Machines Engineering Department, Faculty of Engineering at Tanta. His research interests include the steady state and transient stability of HVDC systems, FACTS, load forecasting, multi-level inverters, dissolved gas analysis, power transformer health index, artificial intelligent technique applications, PV system fault detection, and distance adaptive protective relays.

FADY WADIE received the B.Sc. degree in electrical power engineering from Ain Shams University, in 2009, and the M.Sc. and Ph.D. degrees in high voltage engineering from Benha University (Shoubra Branch), Cairo, in 2015 and 2019, respectively. He is currently a Lecturer with Egyptian Russian University. His research interests include the switching transients of circuit breakers and their mitigation, wide area back-up protection, and fault detection algorithms based on communication assisted techniques.